RESEARCH ARTICLE

Identification and activity of acetate-assimilating bacteria in diffuse fluids venting from two deep-sea hydrothermal systems

Matthias Winkel[1], Petra Pjevac[1], Manuel Kleiner[2], Sten Littmann[3], Anke Meyerdierks[1], Rudolf Amann[1] & Marc Mußmann[1]

[1]Department of Molecular Ecology, Max Planck Institute for Marine Microbiology, Bremen, Germany; [2]Department of Symbiosis, Max Planck Institute for Marine Microbiology, Bremen, Germany and [3]Department of Biogeochemistry, Max Planck Institute for Marine Microbiology, Bremen, Germany

Correspondence: Marc Mußmann and Petra Pjevac, Department of Molecular Ecology, Max Planck Institute for Marine Microbiology, Bremen, Germany. Tel.: +49 421 2028 936; fax: +49 421 2028 580; e-mail: mmussman@mpi-bremen.de

Present address: Matthias Winkel, Geomicrobiology Section, Helmholtz Centre Potsdam, GFZ German Research Centre for Geosciences, Potsdam, Germany

Received 28 July 2014; revised 10 September 2014; accepted 16 September 2014. Final version published online 13 October 2014.

DOI: 10.1111/1574-6941.12429

Editor: Tillmann Lueders

Keywords
Epsilonproteobacteria; *Gammaproteobacteria*; heterotrophy; 16S rRNA gene; nanoSIMS; stable isotopes.

Abstract

Diffuse hydrothermal fluids often contain organic compounds such as hydrocarbons, lipids, and organic acids. Microorganisms consuming these compounds at hydrothermal sites are so far only known from cultivation-dependent studies. To identify potential heterotrophs without prior cultivation, we combined microbial community analysis with short-term incubations using ^{13}C-labeled acetate at two distinct hydrothermal systems. We followed cell growth and assimilation of ^{13}C into single cells by nanoSIMS combined with fluorescence *in situ* hybridization (FISH). In 55 °C-fluids from the Menez Gwen hydrothermal system/Mid-Atlantic Ridge, a novel epsilonproteobacterial group accounted for nearly all assimilation of acetate, representing the first aerobic acetate-consuming member of the *Nautiliales*. In contrast, *Gammaproteobacteria* dominated the ^{13}C-acetate assimilation in incubations of 37 °C-fluids from the back-arc hydrothermal system in the Manus Basin/Papua New Guinea. Here, 16S rRNA gene sequences were mostly related to mesophilic *Marinobacter*, reflecting the high content of seawater in these fluids. The rapid growth of microorganisms upon acetate addition suggests that acetate consumers in diffuse fluids are copiotrophic opportunists, which quickly exploit their energy sources, whenever available under the spatially and temporally highly fluctuating conditions. Our data provide first insights into the heterotrophic microbial community, catalyzing an under-investigated part of microbial carbon cycling at hydrothermal vents.

Introduction

In submarine hydrothermal systems, inorganic carbon is the primary carbon source (Shively *et al.*, 1998; Nakagawa & Takai, 2008). However, diffuse and end-member hydrothermal fluids can also contain various organic compounds other than methane (Holm & Charlou, 2001; Rogers & Amend, 2006; Konn *et al.*, 2009; Charlou *et al.*, 2010; Lang *et al.*, 2010; Reeves *et al.*, 2014). Organic acids, lipids, and hydrocarbons are formed in the deep subsurface by serpentinization and subsequent Fischer–Tropsch-type processes under elevated temperature and pressure (Shock & Schulte, 1998; Holm & Charlou, 2001). Furthermore, simple organic compounds are formed by thermal decomposition of biomass (McCollom & Seewald, 2007), homoacetogenesis (Drake *et al.*, 2008; Lever *et al.*, 2010) or by the vent-associated macrofauna (Pimenov *et al.*, 2002). Thus, elevated concentrations (3–35 μmol L^{-1}) of formate and acetate have been measured in venting fluids from shallow and deep-sea hydrothermal systems (Amend *et al.*, 1998; Lang *et al.*, 2010).

Early cultivation-independent studies showed that radioactively labeled acetate and glucose were consumed by yet unknown microorganisms in (diffuse) hydrothermal fluids of the Galapagos Rift (Tuttle *et al.*, 1983), the East Pacific Rise (Tuttle, 1985), the Guaymas Basin (Karl *et al.*, 1988; Bazylinski *et al.*, 1989), and at the Loihi Seamount (Karl *et al.*, 1989). Beyond these studies, little is known about the microorganisms consuming nonmethane organic carbon at hydrothermal vents. In

cultivation-dependent approaches phylogenetically diverse, mostly thermophilic strains from *Deinococcus-Thermus*, *Thermotogae*, *Proteobacteria, Deferribacterales,* and *Archaea* were shown to thrive on organic carbon (Pley, 1991; Huber *et al.*, 1995; Marteinsson *et al.*, 1995; Raguénès *et al.*, 1996). Genomes of vent-associated *Epsilonproteobacteria* (*Sulfurimonas*/*Sulfurovum*-group, Campbell *et al.*, 2006; Sievert *et al.*, 2007; Yamamoto & Takai, 2011) also indicate a certain potential for organic carbon consumption. It was proposed that these hydrogen- and sulfur-oxidizing lithoautotrophs might use simple organic compounds like acetate as growth supplement (Sievert *et al.*, 2008).

Our objective was to identify microorganisms assimilating organic carbon other than methane in discharged diffuse fluids without prior cultivation. In general, diffuse fluids can cover a large temperature range (2.8 to > 100 °C) and usually consist of seawater mixed with hot end-member fluids (Wankel *et al.*, 2011). For our analysis, we sampled sulfidic, diffuse fluids from two deep-sea hydrothermal systems, the Menez Gwen hydrothermal system at the Mid-Atlantic Ridge (MAR) and the Manus Basin back-arc system off the coast of Papua New Guinea. *In situ* temperatures of the diffuse fluids ranged from 25 to 56 °C (Menez Gwen) and from 4 to 73 °C (Manus Basin). We incubated four different fluids at *in situ* temperatures with ^{13}C-labeled acetate as model compound to follow the assimilation of organic carbon (Wright & Hobbie, 1966; Hoppe, 1978; Berg *et al.*, 2013) and monitored changes in the microbial community by 16S rRNA gene pyrotag-sequencing, 16S rRNA gene clone libraries and fluorescence *in situ* hybridization (FISH). In contrast to previous environmental studies using ^{13}C-labeled tracers (Vandieken *et al.*, 2012; Berg *et al.*, 2013), we applied lower substrate concentrations (10 and 30 μmol L^{-1} acetate) and shorter incubation times (8–12 h) to minimize experimentally introduced bias. Finally, we identified ^{13}C-acetate assimilating populations by combining nanometer scale secondary ion mass spectrometry (nanoSIMS) with FISH. Our approach to combine 16S rRNA gene diversity analysis, single cell identification and nanoSIMS measurements provide insights into the identity and activity of uncultured microorganisms consuming organic carbons in diffuse hydrothermal fluids.

Materials and methods

Site description and sampling

Diffuse fluids from the Menez Gwen hydrothermal vent field (37°50′N, 31°30′W) were sampled in September/October 2010 at 828 m depth during the cruise M82-3 on board of the R/V Meteor. Menez Gwen is a basalt-hosted hydrothermal system located southwest of the Azores on the MAR. We sampled diffusely venting fluids at the site Woody Crack (WC), a fissure in the basalt crust of *c.* 1 m length and 0.2 m width. *In situ* temperatures ranged from 25 to 56 °C with a pH of *c.* 4.9 (Table 1). Additional samples were collected from the hydrothermal plume (WC-P, 23 m above Woody Crack) and from bottom water above a patch of the vent mussel *Bathymodiolus azoricus* (WC-M, Supporting Information, Fig. S1). For a more detailed description of the sampling site see Marcon *et al.* (2013).

Diffuse fluids from the Manus Basin (MB) back-arc spreading center off the coast of Papua New Guinea were recovered in June/July 2011 during cruise SO-216 of the R/V Sonne. Here, we sampled the felsic-hosted hydrothermal vent fields North Su (3°47′S, 152°06′W) and Fenway (3°43′S, 151°40′W). At the North Su (NS), underwater volcano diffuse fluids were recovered from two venting fissures in the seafloor in *c.* 1200 m water depth (NS-I: 16–40 °C, pH *c.* 7.1 and NS-II: 54–73 °C, pH *c.* 3.6). From the smaller vent field Fenway (FW) located northeast of North Su in the PACMANUS area, cold but shimmering diffuse fluids were sampled above a patch of vestimentiferan tube worms in 1706 m depth (3.7 °C, pH *c.* 7.3) (Fig. S1, Table 1).

During both cruises, samples were collected with the remotely controlled flow-through system (Kiel Pumping System – KIPS; Schmidt *et al.*, 2007) mounted onto the remotely operated underwater vehicle ROV Quest (MARUM, Bremen). At Woody Crack, the flasks (675 mL, Savillex) of the KIPS system were prefilled with ambient bottom seawater obtained by a CTD cast. At the Manus Basin sites, flasks were prefilled with de-ionized water, which was exchanged for ambient seawater during the ROV descent. At all sites, the pumping rate was *c.* 1 L min^{-1} and pumping time per sample was set at 3 min ensuring exchange of flask volume by sample volume at least four times. A temperature probe located next to the KIPS sampling nozzle was used to monitor temperature during sampling. Fluid samples from multiple KIPS bottles were combined and divided into subsamples for microbial community analysis, stable isotope (SI)-incubation experiments, and geochemical analysis. Because of the limited fluid volume (< 6 L) that could be retrieved per sampling event, several ROV dives were necessary to recover sufficient fluid volumes for separate experiments at sites Woody Crack and North Su-II (samples WCa-c, NS-IIa, and NS-IIb, Table 1).

Fluid geochemistry

Ammonium concentrations were determined photometrically by nesslerization (Bower & Holm-Hansen, 1980).

Table 1. Sampling sites and chemical characteristics of diffuse fluids

Station	Sample	Location	Depth (m)	Temperature (°C)	pH	NH_4 (μmol L^{-1})	NO_3^- (μmol L^{-1})	H_2S (μmol L^{-1})	Mg^{2+} (μg mL^{-1})	O_2 (mg L^{-1})	O_2 saturation (%)
Woody Crack (Menez Gwen)											
M83-2-702	Woody Crack plume (WC-P)*	N37°50.671 E31°31.150	805	9	n.d.	66.9	22.9	n.d.	n.d.	+†	n.d.
M83-2-719	Woody Crack (WCa)*,‡	N37°50.673 E31°31.154	828	46–56	5.0	7.8	16.3	+§	+§	+†	n.d.
M83-2-736	Woody Crack (WCb)*,¶	N37°50.673 E31°31.158	828	25–49	4.9	5.3	17.4	+§	+§	+†	n.d.
M83-2-754	Woody Crack (WCc)**	N37°50.673 E31°31.154	828	49–68	4.6	n.d.	n.d.	+§	+§	+†	n.d.
M83-2-761	Mussel bed (WC-M)*	N37°50.675 E31°31.155	828	9.3	7.0	n.d.	n.d.	n.d.	n.d.	+†	n.d.
Manus Basin											
SO216-29	Fenway*,‡,¶,** (FW)	S03°43.697 E151°40.350	1706	3.7	7.2	2.6	n.d.	< 5	1110–1185	4.9	45
SO216-21	North Su*,‡,¶,** (NS-I)	S03°47.955 E152°06.080	1200	16–40	7.1	1.9	n.d.	14–66	1071–1096	3.6	84
SO216-45	North Su*,‡,** (NS-IIa)	S03°47.998 E152°06.057	1155	54–73	3.6	10.9	n.d.	113–302	854–928	n.d	n.d
SO216-19	North Su¶ (NS-IIb)	S03°47.998 E152°06.051	1155	59–73	3.1	30.0	n.d.	n.d.	1028–1079	2.2	181

n.d., not determined.

*Used for CARD-FISH analysis.

†Detected by ISMS (S. Hourdez, pers. commun.).

‡Used for aerobic ^{13}C-acetate incubations, molecular and isotopic analysis (CARD-FISH, 16S rRNA gene libraries, IRMS, nanoSIMS).

¶Used for 16S rRNA gene pyrotag analysis.

§Data will be published elsewhere by E.P. Reeves.

**Used for acetate-free and anoxic control experiments.

Nitrate was measured according to Braman & Hendrix (1989) using a CLD 60 NO_x analyzer (Eco Physics). Total dissolved sulfide was determined spectrophotometrically in zinc acetate fixed samples as described in Cline (1969). Acetate concentrations in Woody Crack fluids were only measured by high pressure liquid chromatography (HPLC) in the home laboratory. Acetate in Manus Basin fluids was detected at the sampling site by *in situ* mass spectrometry (ISMS) at AMU 60 (Bach, 2011) and was also measured by 2D-high-pressure ion chromatography (HPIC, ICS-5000 HPIC, Thermo Scientific, Darmstadt, Germany) in the home laboratory. Oxygen concentrations and pH data for Manus Basin diffuse fluids (Table 1) were measured on board directly after fluid retrieval, while reported Mg^{2+} concentrations represent preliminary data obtained by ion chromatography (IC) measurements in the home laboratory (data kindly provided by C. Breuer). Detailed geochemical data will be published elsewhere by E.P. Reeves and A. Koschinsky.

16S rRNA gene pyrotag diversity analyses in diffuse hydrothermal fluid samples

For 16S rRNA gene diversity analyses, we filtered diffuse fluids (samples WCb, FW, NS-I and NS-IIb, Table 1) through polyethersulfone (PES) membranes (0.22 μm pore size, Milipore, Darmstadt, Germany) attached to the KIPS system. Membranes were stored at −80 °C until DNA was extracted with the Ultra Clean Soil DNA Kit (MoBio Laboratories, Carlsbad) as instructed in the manual. Bacterial 16S rRNA genes were amplified by PCR with primers GM3F and 907RM (Muyzer *et al.*, 1995, 1998) in ten parallel reactions using the Phusion High Fidelity DNA Polymerase (NEB, Ipswich). PCR products were pooled, gel purified and 454-pyrosequenced at the Max Planck Genome Center (Cologne, Germany). Further details on PCR and sequencing are provided in the Methods S1. Sequence reads > 200 bp were analyzed with the bioinformatics pipeline of the SILVA database project (Quast *et al.*, 2013) as described in Klindworth *et al.* (2013). Descriptive sequence statistics are presented in Table S1.

^{13}C-acetate and ^{15}N-ammonium incubations

We used 330 mL of diffuse fluids from Woody Crack (Menez Gwen) for onboard stable isotope (SI)-incubations in 1000 mL (at Menez Gwen) glass bottles. For experiments with fluids from the Manus Basin, we used 150 mL of fluids in 500 mL glass bottles. For oxic experiments the headspace was air, while for anoxic incubations fluids and headspace were flushed with N_2/CO_2 (80/20) for several minutes. To allow re-adaption of microorganisms, the fluids were pre-incubated at *in situ* temperature for 1 h before addition of ^{13}C-acetate and ^{15}N-ammonium. To diffuse fluids from Woody Crack (WCa, WCc), we added sodium 1-^{13}C-acetate (99 atom-percent ^{13}C [AT% $^{13}C = (^{13}C/(^{13}C + ^{12}C)) \times 100$], Sigma-Aldrich) at a final concentration of 10 μmol L^{-1}. For incubations of fluids from the Manus Basin (FW, NS-I, NS-IIa), we increased ^{13}C-acetate concentrations to 30 μmol L^{-1} to ensure sufficient labeling, as onboard ISMS detected a compound with the atomic mass unit 60 that possibly was acetic acid (Bach, 2011). To all incubations, we also added ^{15}N-ammonium chloride (98 AT% ^{15}N [AT% $^{15}N = (^{15}N/(^{15}N + ^{14}N)) \times 100$], Sigma-Aldrich) as a general activity marker at a final concentration of 10 μmol L^{-1}. As live controls oxic and anoxic incubations were set up to which no ^{13}C-acetate was added. For dead controls, we added formaldehyde (final concentration 1%) to substrate-amended diffuse fluids. For each experimental set up duplicate (FW, NS-I, NS-IIa) or triplicate (WCa) incubations were performed. Fluids were incubated at *in situ* temperatures for 8 h (55 °C, WCa and 72 °C, NS-IIa), 10 h (37 °C, NS-I), or 12 h (4 °C, FW). Incubations were stopped by addition of formaldehyde (final concentration 1%) and fixed for 1 h at room temperature. From each bottle, 50–100 mL aliquots were filtered on a glass fiber filter (type GF, 0.7 μm pore size, Millipore, Darmstadt, Germany) for bulk SI measurements. The remaining volume was filtered on multiple gold-palladium coated polycarbonate membranes (type GTTP, 0.2 μm pore size, Millipore, Darmstadt, Germany) for nanoSIMS and CARD-FISH analyses. All filters were air-dried and stored at −20 °C.

Isotope ratio mass spectrometry (IRMS)

For bulk measurements of ^{13}C and ^{15}N content, GF filters were analyzed by gas chromatography-isotope ratio mass spectrometry (GC-IRMS). Before combustion, GF filters were decalcified in a hydrochloric acid (37%) atmosphere for 24 h in a desiccator (Musat *et al.*, 2008). Then the isotope abundance was measured in the released CO_2 and N_2 after flash-combustion of GF filters in excess oxygen at 1050 °C in an automated elemental analyzer (Thermo Flash EA, 1112 Series, CE Elantech, Lakewood, NJ) coupled to a Delta Plus Advantage mass spectrometer (Finnigan, Thermo Fisher Scientific, Waltham, MA).

Total cell counts (TCC) and CARD-FISH

For TCC and CARD-FISH counts, 100 mL of diffuse fluids and of the hydrothermal plume were formaldehyde-fixed on board (final concentration 1%, overnight at

4 °C) and filtered on polycarbonate membrane filters (type GTTP, 0.2 μm pore size, 25 mm filter diameter, Millipore, Darmstadt, Germany). For TCC, cells were stained with 4′,6-diamidino-2-phenylindole (DAPI). CARD-FISH was performed as described earlier (Ishii *et al.*, 2004; Teira *et al.*, 2004). Details of the applied oligonucleotide probes are listed in Table S2. For double hybridizations, filters were consecutively hybridized with two probes (Pernthaler *et al.*, 2004) using Alexa488 and Alexa594 fluorochromes (Invitrogen, Karlsruhe, Germany).

Marking and mapping of hybridized cells for nanoSIMS

To combine CARD-FISH identification of single cells with nanoSIMS analysis, we used correlative microscopy. The position of cell assemblages identified by CARD-FISH on the filter was marked using a laser (Laser Microdissection Microscope, DM6500B, Leica, Wetzlar, Germany). Fields of view with a suitable distribution of hybridized cells were marked with numbers, arrows, and borders to guarantee recovery of cells during nanoSIMS analysis. Microscopic images were taken for orientation purpose during the nanoSIMS analysis and for postprocessing with the LOOK@NANOSIMS software (Polerecky *et al.*, 2012).

NanoSIMS analysis

Hybridized cells within the marked areas on the filters were analyzed with a nanoSIMS 50L instrument (Cameca, Gennevilliers, Cedex-France). Secondary ions $^{12}C^-$, $^{13}C^-$, $^{12}C^{14}N^-$, $^{12}C^{15}N^-$, and $^{32}S^-$ were simultaneously recorded for each individual cell using five electron multipliers. Samples were presputtered with a Cs^+ primary ion beam of 400–500 pA to remove surface contaminations, to implant Cs^+ ions and to achieve a stable ion emission rate. During analysis, the samples were sputtered with a 0.8–1.8 pA Cs^+ primary ion beam focused into a spot of 50–100 nm diameter that was scanned over an analysis area of 5 × 5 μm to 30 × 30 μm with an image size of 256 × 256 pixel or 512 × 512 pixel and a counting time of 1 ms per pixel. The individual masses were tuned for high mass resolution (around 7000 MRP). Respective mass peaks were tuned directly on the sample. Depending on the fields of view (5 × 5 μm to 30 × 30 μm), between 20 and 100 planes were recorded.

The measured data were processed using the LOOK@NANOSIMS software (Polerecky *et al.*, 2012). The images of one field of view recorded during one measurement were drift corrected and accumulated. Regions of interest (ROI) corresponding to individual cells were defined using images of $^{12}C^-$, $^{12}C^{14}N^-$, and $^{32}S^-$. For each ROI $^{13}C/(^{13}C + ^{12}C)$, $^{12}C^{15}N/(^{12}C^{15}N + ^{12}C^{14}N)$, and $^{32}S/^{12}C$ ratios were calculated. Ratios with more than 10% trend (increase or decrease) with depth were excluded from further analysis.

Calculation of assimilation per biovolume

Assimilation of ^{13}C and ^{15}N per biovolume was calculated for 135 cells from Woody Crack fluids (Menez Gwen), for 35 cells from FW and for 65 cells from NS-I fluids (Manus Basin). Most cells were rod-shaped, and cell volume was calculated based on measured values of cell diameters and cell lengths by adding up the respective volumes of a sphere and a cylinder. For biovolume-to-biomass conversion, we used a calibration factor of 0.38 pg C μm^{-3} known for small heterotrophic bacteria (Lee & Fuhrman, 1987). The calculated biomasses were correlated with the $^{13}C/(^{13}C + ^{12}C)$ ratio and corrected for dead control bulk measurements, assuming that only ^{13}C-labeled acetate was present in the incubations, as we could not detect natural acetate in fluids (100%-labeling). The nitrogen content of cells was calculated based on a conversion factor of 3.7 for C: N mass ratio for heterotrophs (Lee & Fuhrman, 1987), correlated with the $^{15}N/(^{15}N + ^{14}N)$ ratio and corrected for bulk measurement of dead controls.

16S rRNA gene libraries and phylogenetic analyses

Bacterial 16S rRNA genes were amplified by filter-PCR (Kirchman *et al.*, 2001) or from filter-extracted DNA (Ultra Clean Soil DNA Kit, MoBio Laboratories, Carlsbad) of formaldehyde-fixed samples collected at the end of ^{13}C-acetate incubations. Primers GM3F and GM4R, (Muyzer *et al.*, 1995) or primers GM5F (Muyzer *et al.*, 1995) and 907RM were applied. After gel purification, PCR products were cloned and Sanger-sequenced. Further details are given in the Methods S1.

Phylogenetic analysis was performed with the ARB software package (Ludwig *et al.*, 2004) based on a sequence alignment with the SINA aligner (Pruesse *et al.*, 2012) against the SILVA 16S rRNA SSU reference database, release 111 (Quast *et al.*, 2013). Phylogenetic trees were calculated with nearly full-length sequences (> 1400 bp) using a 50% conservation filter and the maximum likelihood algorithm RAXML with 100 bootstraps (Stamatakis *et al.*, 2005) implemented in ARB. Nucleotide substitutions were weighted according to the GTR model (Lanave *et al.*, 1984). Partial sequences were added to the tree using the maximum parsimony algorithm without allowing changes in tree topology.

Nucleotide sequence accession numbers

Nucleotide sequences from this study were deposited in the EMBL, GenBank, and DDBJ nucleotide database with the accession numbers HG962423–HG962430 for full-length sequences and HG819042–HG819115 for partial sequences from Menez Gwen, and HG818825–HG819041 for partial sequences from Manus Basin. The 16S rRNA gene pyrotag sequences have been deposited at Sequence Read Archive under sample accession numbers ERS377555–ERS377558.

Results

Geochemistry of diffuse hydrothermal fluids

Diffuse fluids sampled at Woody Crack (Menez Gwen, MAR) consisted of 100% seawater that interacted with a vaporous phase enriched in reduced compounds (Reeves *et al.*, 2011). The fluids displayed the typical sulfidic odor, which is in line with previous measurements of 1.7 mmol kg^{-1} sulfide in other Menez Gwen fluids (Charlou *et al.*, 2000), indicating hydrothermally influenced fluids. Furthermore, modeling revealed 60 mmol kg^{-1} sulfide above mussel patches surrounding Woody Crack (Marcon *et al.*, 2013). Acetate was not detected by 2D-HPIC at a detection limit of 1 μmol L^{-1}. Ammonium concentrations in fluids ranged from 5 to 8 μmol L^{-1}. Nitrate concentrations were between 16 and 18 μmol L^{-1} (Table 1). Oxygen was detected by ISMS only qualitatively (S. Hourdez, pers. commun.).

For the diffuse fluids in the Manus Basin end-member hydrothermal fluid accounted for 8% (Fenway, FW) to 30% (North Su-II, NS-II) (Table 1). These values were calculated from Mg^{2+} concentrations in diffuse fluids (Table 1), standard seawater Mg^{2+} concentration (1286.2 μg mL^{-1}), and the generally assumed absence of Mg^{2+} in end-member hydrothermal fluids. In the 4 °C fluid (FW, Manus Basin), sulfide concentrations were close to the detection limit (*c.* 2 μmol L^{-1}), while 14–66 μmol L^{-1} were detected in the 37 °C (NS-I) and 113–302 μmol L^{-1} in the 72 °C (NS-IIa) fluid (Table 1). Ammonium concentrations ranged from 1.9 μmol L^{-1} (FW, NS-I) to up to 30 μmol L^{-1} (NS-IIa). Oxygen ranged from 2.2 to 4.9 mg L^{-1} (Table 1), equaling saturation values from 45 to > 100%. While acetic acid was possibly detected by ISMS measurements in fluids from Manus Basin (Bach, 2011), exact acetate measurements by 2D-HPIC were hampered by strong background of other, yet unknown compounds. For all diffuse fluids sampled in this study, detailed geochemical data will be published elsewhere by E.P. Reeves and A. Koschinsky. All chemical data clearly indicated a hydrothermal contribution to the fluid composition.

Microbial community composition in diffuse fluids from Woody Crack (Menez Gwen)

To characterize the microbial community and to identify potential organic carbon-consuming microorganisms in the 55 °C diffuse fluid at Woody Crack, we determined TCC and conducted CARD-FISH and 16S rRNA gene pyrotag sequencing. TCC were $1.6 \pm 0.3 \times 10^5$ cells mL^{-1}, of which 99% were identified as *Bacteria* by CARD-FISH (Table S3). Bacterial 16S rRNA gene pyrotags (6798 reads) were dominated by *Epsilonproteobacteria* (51% of all reads, Fig. 1), which accounted for 10% of TCC (Fig. 2 and Table S3). *Gammaproteobacteria* accounted for 10% of 16S rRNA gene pyrotags, but made up 65% of TCC. Here, it has to be taken into account that two different fluids samples were used for CARD-FISH and pyrotag analysis (Table 1). The observed discrepancies could reflect the highly dynamic nature of the sampled vents. Moreover, most epsilonproteobacterial genomes encode 3–4 rRNA operons, possibly leading to an overrepresentation of *Epsilonproteobacteria* in sequence data. Moreover, samples for pyrotags and FISH experiments were retrieved from separate ROV dives (Table 1). *Alphaproteobacteria* accounted for 18%, while all other bacterial groups made up < 5% of 16S rRNA gene pyrotags.

The majority (85%) of epsilonproteobacterial pyrotags was related to the mesophilic, lithoautotrophic genera *Sulfurimonas*, *Sulfurovum,* and *Arcobacter* within the order *Campylobacterales* (Fig. 1). These genera are often dominant members in sulfidic, hydrothermal environments in the deep-sea (Campbell *et al.*, 2006; Sievert *et al.*, 2007). *Nautiliales* constituted 10% of epsilonproteobacterial 16S rRNA gene pyrotags (Fig. 1). This order harbors metabolically diverse organisms including mixo- and autotrophic thermophiles (Campbell *et al.*, 2001, 2006; Miroshnichenko *et al.*, 2002). Most of the gammaproteobacterial pyrotags were affiliated with sequences from *Oceanospirillales* (e.g. SUP05) and *Alteromonadales* (e.g. *Psychromonas*).

Microbial community composition in diffuse fluids from the Manus Basin

Although the three diffuse fluids from the Manus Basin covered a large temperature range (4, 37 and 72 °C), TCC were similar and ranged from 2.2 to 6.2×10^4 cells mL^{-1} (Fig. 2, Table S3). *Bacteria* accounted for 58–85% and *Archaea* for 8–11% of TCC (Table S3). In total, 10 516 bacterial 16S rRNA gene pyrotags were recovered.

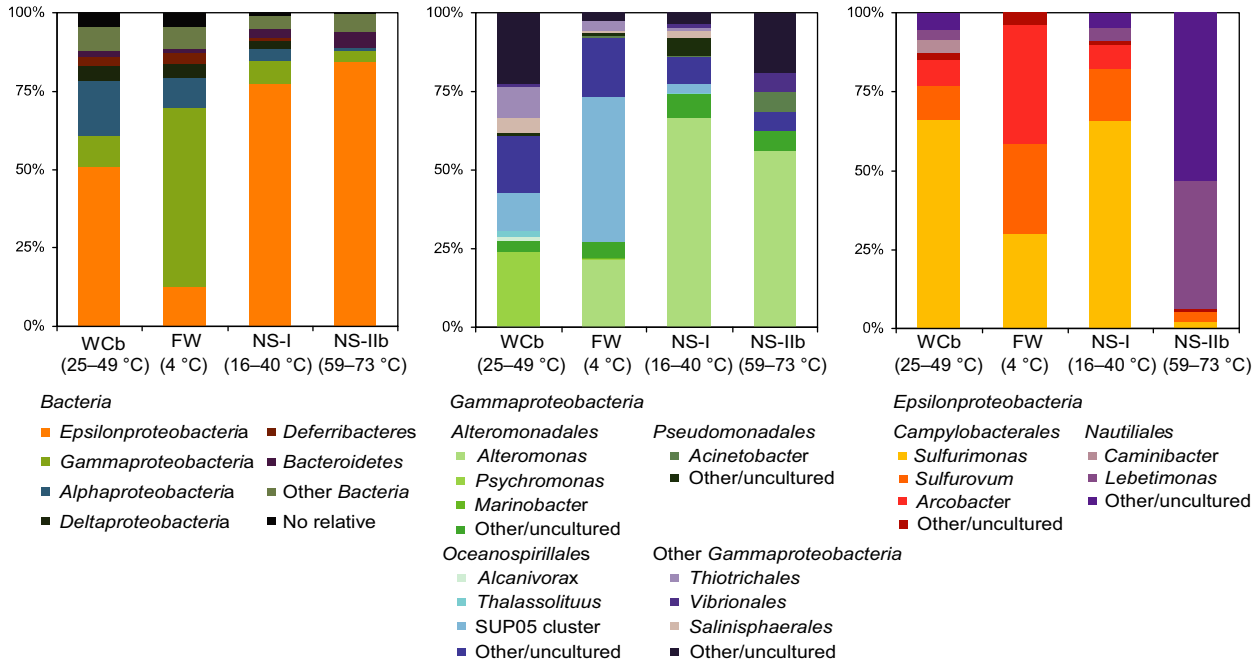

Fig. 1. Diversity of the bacterial community analyzed by 16S rRNA gene pyrotags in diffuse fluids from Woody Crack (WCb), Fenway (FW), North Su-I (NS-I), and North Su-IIb (NS-IIb).

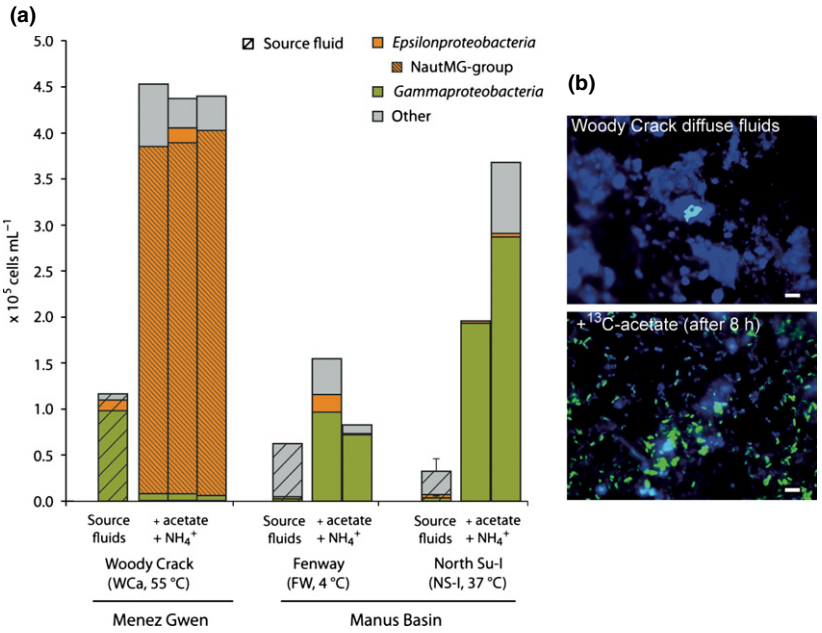

Fig. 2. (a) TCC and abundances (CARD-FISH) of *Gammaproteobacteria* and *Epsilonproteobacteria* in diffuse fluids (WC, FW, and NS-I) and in oxic acetate/ammonium incubations. Triplicates were counted in incubations from Woody Crack fluids (WCa) and source diffuse fluids from North Su-I, while duplicates were counted for Fenway and North Su-I incubations. Other samples were not counted in replicates. (b) Epifluorescent images of NautMG-cells (green fluorescence) by probe Naut842 in diffuse fluids (upper panel) and in ^{13}C-acetate/ammonium incubation experiments (lower panel) using CARD-FISH. Scale bars represent 5 μm.

In all samples *Proteobacteria* clearly dominated the communities, accounting for 84–91% of pyrotags (Fig. 1). In the 4 °C fluids (FW), *Gammaproteobacteria* made up 57% of pyrotags, whereas they contributed only 4% of TCC (Fig. 2, Table S3). Numerous sequences were related to the SUP05 clade (Fig. 1), which it is not targeted by

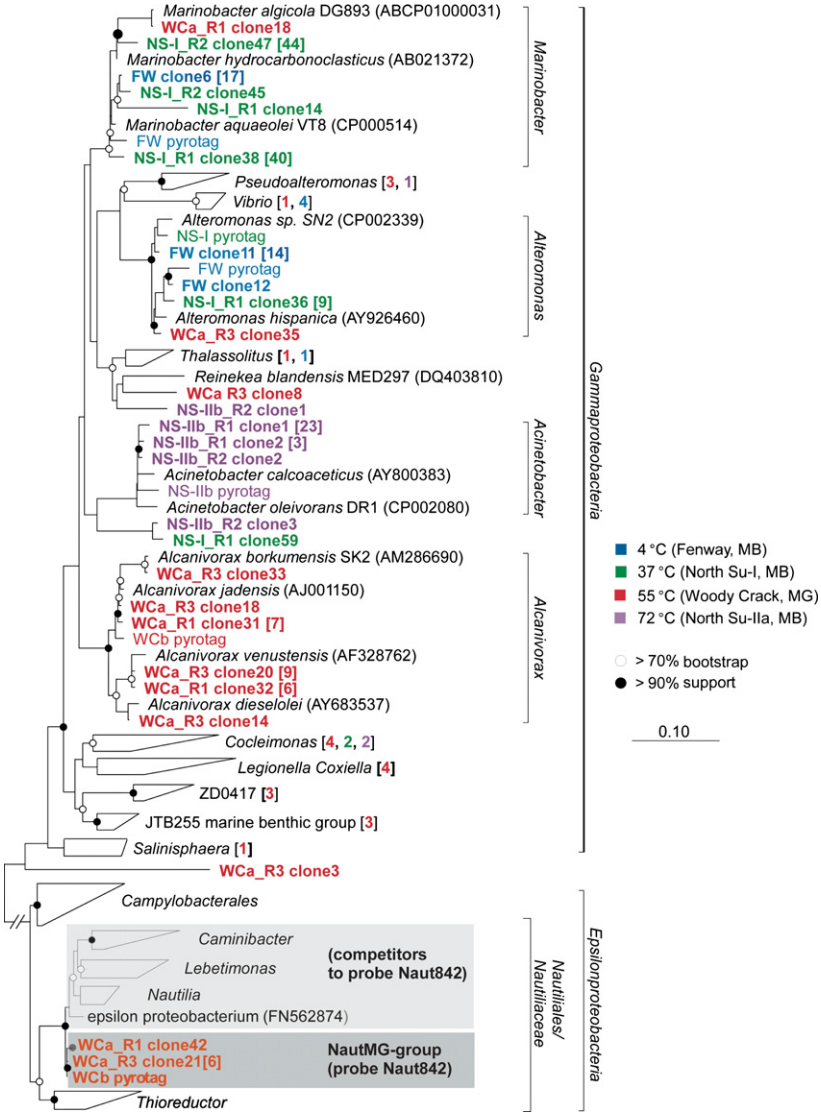

Fig. 3. Phylogenetic reconstruction of 16S rRNA gene sequences of *Gammaproteobacteria* and *Epsilonproteobacteria* in diffuse fluids (pyrotags) from Woody Crack (Menez Gwen), from the three Manus Basin fluids and from ^{13}C-acetate incubation experiments (clones). The dark gray rectangle indicates the NautMG-group targeted by probe Naut842. The light dark rectangle indicates groups targeted by competitors to probe Naut842. Numbers of sequences per OTU (97% sequence identity cut-off) are given in parenthesis. Scale bar represents 10% estimated sequence divergence.

the general probe Gam42a, thus leading to an underestimation of the abundance of *Gammaproteobacteria* by CARD-FISH. Some sequences grouped with heterotrophic genera such as *Acinetobacter, Marinobacter,* and *Alteromonas* (Fig. 3). *Epsilonproteobacteria* (all *Campylobacterales*) accounted for 12% of 16S rRNA gene pyrotags (Fig. 1) and for 4% of TCC (Table S3).

In both fluid samples from the North Su vent field (37 °C, NS-I and 72 °C, NS-IIb) *Epsilonproteobacteria* constituted the major fraction of 16S rRNA gene pyrotags (78–85%), whereas CARD-FISH indicated abundances of 7–15% of TCC (Table S3). Again, this discrepancy is possibly caused by the higher rRNA operon number in epsilonproteobacterial genomes or possibly by different community compositions as a consequence of separate sample collections at NS-II (Table 1). In the 37 °C fluid sample, (NS-I) the majority of all epsilonproteobacterial sequences (90%) was related to the *Campylobacterales*, while sequences related to the *Nautiliales* represented a minor fraction (9% of epsilonproteobacterial sequences). In contrast, > 93% of epsilonproteobacterial sequences from the 72 °C fluid (NS-IIb) were classified as *Nautiliales* (Fig. 1). According to CARD-FISH results, *Gammaproteobacteria* were similarly abundant (5–15%) as *Epsilonproteobacteria* (Table S3) and made up 4–7% of 16S rRNA gene pyrotags in NS-I and NS-IIb fluids. The gammaproteobacterial pyrotags were also related to *Acinetobacter* and to *Alteromonas* (Fig. 3).

Acetate-assimilation by *Epsilonproteobacteria* in diffuse fluids from Woody Crack

To identify microbial populations that actively assimilate organic carbon in fluids from Woody Crack (WCa), we

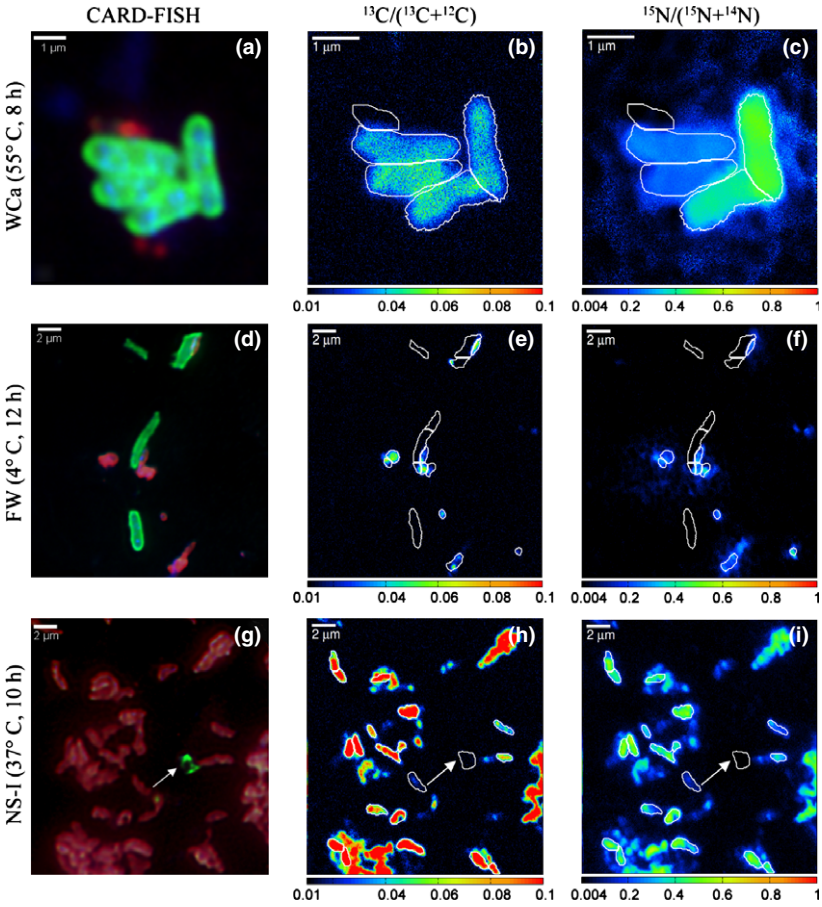

Fig. 4. NanoSIMS images of ^{13}C-acetate and ^{15}N-ammonium uptake by single cells in incubation experiments at Menez Gwen and Manus Basin. Upper row: (a–c) Woody Crack (WCa, 55 °C, 8 h). Middle row (d–f): Fenway (FW, 4 °C, 12 h). Lower row (g–i): North Su (NS-I, 37 °C, 10 h). Left column (a, d, g) CARD-FISH images: *Epsilonproteobacteria* were detected by green and *Gammaproteobacteria* by red fluorescence. Middle column (b, e, h): carbon isotope ratio $^{13}C/(^{13}C+^{12}C)$. Right column (c, f, i): Nitrogen isotope ratio $^{15}N/(^{15}N+^{14}N)$.

followed the assimilation of the model compound ^{13}C-acetate in bulk samples (Fig. S2, Table S4) and in individual cells (Figs 4 and 5) using short-term experiments at *in situ* temperature (55 °C). Besides ^{13}C-acetate, we also added ^{15}N-ammonium as a general activity marker. TCC only increased in incubations with oxic headspace, while TCC did not change in anoxic ^{13}C-acetate and acetate-free control incubations (Fig. 2, Table S3). Bulk ^{13}C- and ^{15}N-content in oxic incubations was higher than in the dead controls (0.8–1.1 excess AT% ^{13}C and 19.1–25.3 excess AT% ^{15}N, respectively), while in anoxic ^{13}C-acetate and acetate-free control incubations ^{13}C- and/or ^{15}N-content were not elevated (Fig. S2, Table S4). These results indicated that ^{13}C-acetate and ^{15}N-ammonium were assimilated into cell material only under oxic conditions.

During the 8 h of incubation the community significantly shifted from a *Gammaproteobacteria*-dominated (65% of TCC in diffuse fluids) to an *Epsilonproteobacteria*-dominated community (86% of TCC) (Fig. 2; Table S3). The *Epsilonproteobacteria* grown in oxic ^{13}C-acetate incubations were further identified by 16S rRNA gene sequencing and CARD-FISH. Almost all retrieved epsilonproteobacterial sequences were affiliated to the family *Nautiliaceae* and formed a separate branch with 94.2% sequence identity to *Nautilia profundicola* (Fig. 3). We designated this novel sequence cluster as 'NautMG-group'. The large majority of gammaproteobacterial clone sequences recovered from this experiment affiliated with the heterotrophic genus *Alcanivorax* (Fig. 3). To quantify the NautMG-group *Epsilonproteobacteria* in incubations and diffuse fluids, we designed the specific oligonucleotide probe Naut842 (Fig. 3, Table S2). This probe targeted 84–87% of TCC in all triplicate oxic ^{13}C-acetate incubations (Fig. 2), indicating that the large majority of epsilonproteobacterial cells grown on ^{13}C-acetate indeed belonged to the NautMG-group. In the source diffuse fluids (WCa), the NautMG-cells made up 0.8% of TCC (Fig. 2, Table S3), in bottom waters above a nearby *Bathymodiolus*-mussel bed (WC-M) they accounted for 0.3% (not shown), but were not detectable in the hydrothermal plume obtained from 23 m above Woody Crack (WC-P). During the 8 h incubation, the abundance of the NautMG-group multiplied by 290-fold and increased from 1.3×10^3 to 3.8×10^5 cells mL^{-1} (Table S3, Fig. 2), equaling a generation time of *c.* 42 min. For *Gammaproteobacteria,* no net-growth was observed and

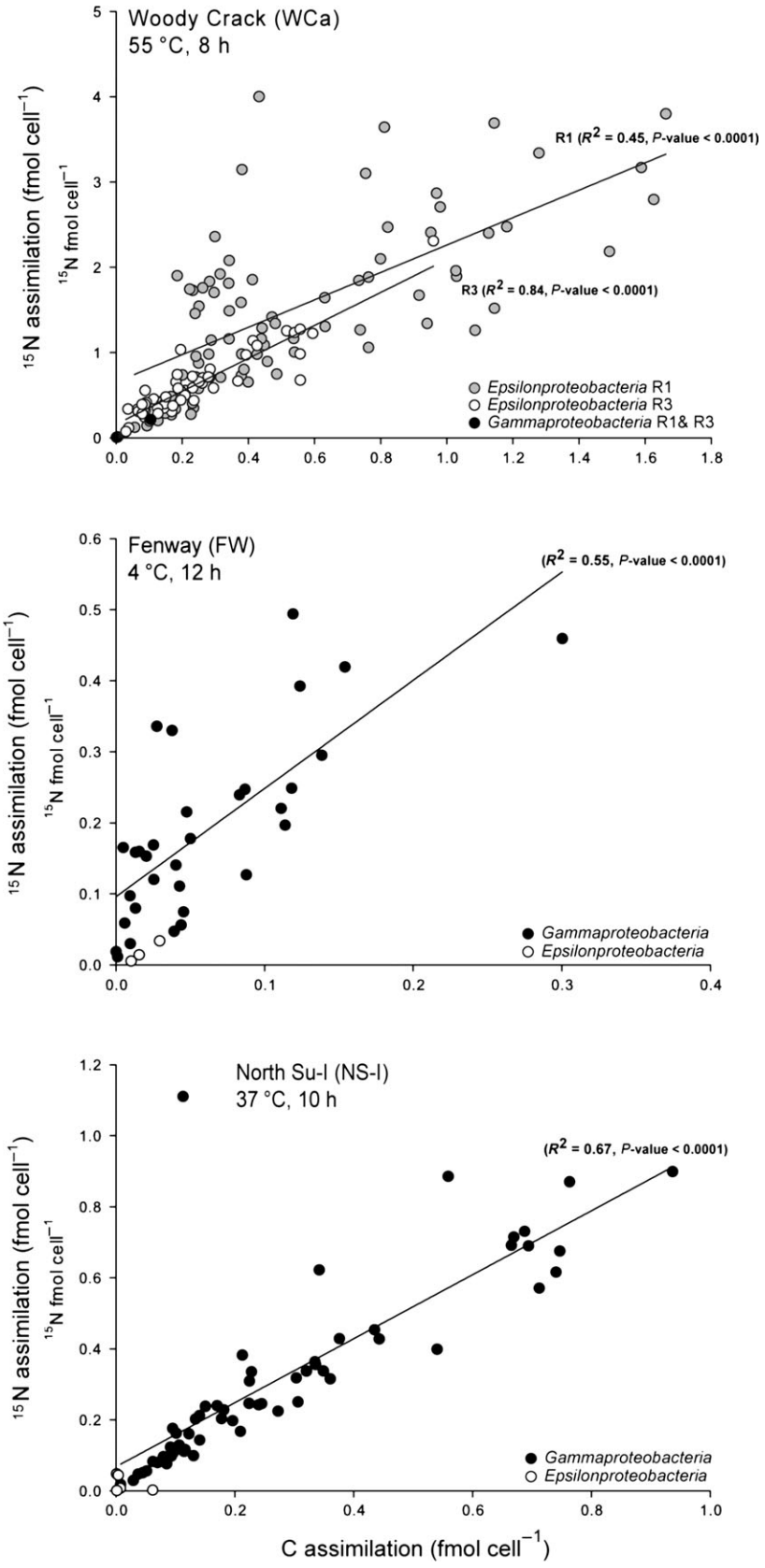

Fig. 5. NanoSIMS analysis of ^{13}C-acetate and ^{15}N-ammonium assimilation by single cells of *Gammaproteobacteria* and *Epsilonproteobacteria*. Upper row: Woody Crack (WCa, 55 °C). Middle row: Fenway (FW, 4 °C). Lower row: North Su-I (NS-I, 37 °C). Scatter plot shows assimilation rates in fmol cell^{-1} after 8 h (WCa), 12 h (FW) or 10 h (NS-I) incubation. The significance level of linear regression analysis was < 0.05.

abundances of FISH-detectable cells declined in ^{13}C-acetate incubations (Fig. 2, Table S3).

We selected two of the triplicate incubations (WCa-R1, WCa-R3) to confirm a consumption of ^{13}C-acetate by the NautMG-group using nanoSIMS. Epsilonproteobaterial and gammaproteobacterial cells (135 cells in total) were identified by CARD-FISH before nanoSIMS analyses. Correlative microscopy and nanoSIMS showed that all analyzed epsilonproteobacterial cells ($n = 132$) clearly incorporated ^{13}C and ^{15}N, whereas the few gammaproteobacterial cells found ($n = 3$) incorporated little or no label (Figs 4 and 5, Fig. S4). Epsilonproteobacterial cells displayed large differences in ^{13}C- and ^{15}N-assimilation per biovolume. Most cells ($n = 89$) showed both relatively low ^{13}C (0.03–0.8 fmol cell^{-1}) and low ^{15}N (0.12–1.4 fmol cell^{-1}) incorporation. Twenty-two cells showed high ^{15}N (up to 4.0 fmol cell^{-1}), but low ^{13}C assimilation (< 0.8 fmol cell^{-1}). Nineteen cells assimilated both high ^{15}N (up to 3.8 fmol cell^{-1}) and high ^{13}C (up to 1.7 fmol cell^{-1}, Fig. 5), when compared to the average ^{15}N and ^{13}C assimilation (^{15}N: 1.2 ± 0.9 fmol cell^{-1}, ^{13}C: 0.4 ± 0.4 fmol cell^{-1}).

Acetate-assimilation by *Gammaproteobacteria* in Manus Basin diffuse fluids

Similar incubations with ^{13}C-acetate and ^{15}N-ammonium were performed with diffuse fluids from three sites at the Manus Basin hydrothermal system (FW, NS-I, NS-IIa). In the oxic 4 and 37 °C incubations, bulk content of ^{13}C and ^{15}N was higher than in anoxic incubations and dead controls (Fig. S2, Table S4). In the oxic 72 °C incubation, bulk content of ^{13}C and ^{15}N was not clearly higher than in the dead controls (Fig. S2).

In the oxic 4 °C (FW) and 37 °C (NS-Ia) ^{13}C-acetate incubations, the TCC increased up to 11-fold, while TCC in anoxic incubations and acetate-free controls did not change or changed only slightly (Fig. 2, Table S3). At both temperatures, the observed growth could be attributed to *Gammaproteobacteria,* which were the most abundant group after incubations (Fig. 2, Table S3). For the 4 °C incubations, this was supported by a 16S rRNA gene library that was dominated by sequences of the seawater-associated and heterotrophic genera *Alteromonas* and *Marinobacter* (Fig. 3). Notably, both gene libraries from duplicates of the 37 °C incubations were dominated by *Marinobacter hydrocarbonoclasticus* (98–99.7% sequence identity) and also contained few sequences related to *Alteromonas marina* (99–99.6%). Here, *Gammaproteobacteria* multiplied in average by 64-fold (Fig. 2).

In the 72 °C incubations (NS-II), TCC decreased in anoxic ^{13}C-acetate and in oxic, acetate-free controls, whereas they were slightly increased in oxic ^{13}C-acetate incubations (Table S3). Cells could not be further identified by CARD-FISH, most likely because of an over-fixation with formaldehyde at 72 °C. The 16S rRNA gene library of the nanoSIMS-analyzed replicate exclusively contained sequences with 94–99.9% sequence identity to the *Acinetobacter* species (Fig. 3). Archaeal 16S rRNA genes could not be amplified from the 72 °C incubations.

The incorporation of ^{13}C and ^{15}N into single gammaproteobacterial cells was confirmed by nanoSIMS and CARD-FISH (Figs 4 and 5). In the 4 °C fluids, (FW) only little ^{13}C-acetate was assimilated by gammaproteobacterial cells ($n = 32$) with up to 0.3 fmol cell^{-1} ^{13}C. The few identified epsilonproteobacterial cells ($n = 3$) assimilated no or very little ^{13}C and ^{15}N (Figs 4 and 5). In the 37 °C (NS-I) incubation, the cellular ^{13}C-assimilation among gammaproteobacterial cells ($n = 59$) varied strongly and ranged from 0.01 to 0.9 fmol cell^{-1}, while epsilonproteobacterial cells ($n = 6$) assimilated no or little ^{13}C and ^{15}N (Figs 4 and 5). In the 72 °C (FW) incubation, we found few, not-further identifiable cells, clearly enriched in both ^{13}C and ^{15}N (Figs S3 and S4).

Discussion

In our study, we confirm that microbial populations in diffuse hydrothermal fluids assimilate nonmethane organic carbon during short-term incubations over a temperature range from 4 to 72 °C. For a further identification of the active microbiota, we combined nanoSIMS analysis of ^{13}C-acetate assimilating cells with 16S rRNA gene sequencing and CARD-FISH. These molecular methods allowed us to detect community shifts and sufficient SI-labeling in cells after incubation periods of only 8–12 h. The added acetate levels were close to those measured previously at other hydrothermal sites (Lang *et al.*, 2010) or those in pelagic, sulfidic redoxclines (Albert *et al.*, 1995; Ho *et al.*, 2002). Using this approach, we avoided extended incubation times and high substrate levels as generally applied for stable isotope-probing of acetate-assimilating microorganisms in environmental studies (Boschker *et al.*, 1998; Pester *et al.*, 2010; Vandieken *et al.*, 2012; Berg *et al.*, 2013; Miyatake *et al.*, 2013).

Notably, our results complement earlier findings by Tuttle *et al.* (1983) and Karl *et al.* (1989), who observed significant assimilation of acetate in diffuse fluids by unknown microorganisms in long-term incubations. In our study, none of the lithoautotrophic clades frequently observed at hydrothermal vents (*Sulfurimonas*, *Sulfurovum*, SUP05) were stimulated, although even strict autotrophs may use acetate as supplementary carbon source (Wood *et al.*, 2004). Moreover, the facultative autotroph *Sulfurimonas gotlandica* GD1 grows with acetate using nitrate as electron acceptor (Grote *et al.*, 2012). Sulfide

and nitrate were clearly present in all incubations, but no acetate uptake was detected in anoxic incubations. Possibly, concentrations of oxygen and/or acetate used in our experiments were not in the range preferred by these groups and/or the incubation times were too short for switching from lithoautotrophic to heterotrophic growth. Instead, heterotrophic populations less abundant in the diffuse fluids were stimulated.

Acetate-assimilation in diffuse fluids of the Manus Basin

In the 4 °C and 37 °C diffuse fluids from the Manus Basin the microbial communities shifted within 8–12 h from *Epsilonproteobacteria*- to *Gammaproteobacteria*-dominated communities. Here, growth of typical seawater heterotrophs like *Alteromonas* and *Marinobacter* well reflected the high seawater-content (> 70%) and the psychro- to mesophilic temperature range in the studied diffuse fluids. In particular, *Marinobacter* strains are metabolically flexible and use various organic substrates including acetate over a large temperature range (Kaye & Baross, 2000; Handley *et al.*, 2009). Moreover, the dominance of *Marinobacter* in the 37 °C incubations (NS-I) is consistent with the frequent detection of *Marinobacter* in other diffuse fluids, in seawater close to hydrothermal discharges (Huber *et al.*, 2007; Kaye *et al.*, 2011) and other samples of hydrothermal origin (Rogers *et al.*, 2003; Santelli *et al.*, 2008). Their competitive advantage over other acetate-consuming microorganisms in our 37 °C-experiments and their widespread occurrence in seawater surrounding hydrothermal habitats suggests that the *Marinobacter*-group could be an important heterotroph in the vicinity of hydrothermal vents.

In the 72 °C incubation (NS-IIa), we detected acetate-assimilating cells and exclusively recovered sequences of the *Acinetobacter*-group. This suggests that the *Acinetobacter*-group possibly also harbors at least thermo-tolerant members. In support of this, mesophilic *Acinetobacter*-epibionts have been isolated from thermo-tolerant *Alvinella* worms thriving at hydrothermal sites (Jeanthon & Prieur, 1990; La Duc *et al.*, 2007). More importantly, yet-uncultured *Acinetobacter* have been implicated in the degradation of hydrothermally-formed aromatic hydrocarbons in 68 °C-brine pools indicating an activity even under thermophilic conditions (Wang *et al.*, 2011).

Acetate-assimilation in diffuse fluids of Woody Crack/Menez Gwen

At Woody Crack, a yet undescribed epsilonproteobacterial group phylogenetically affiliated with *Nautiliales* was almost exclusively responsible for the measured assimilation of acetate at 55 °C under oxic conditions. It was not stimulated in anoxic incubations or acetate-free controls. To date, all known *Nautiliales* are thermophilic and typically occur at hydrothermally active sites (Campbell *et al.*, 2006). So far, heterotrophic *Nautiliales* are yet unknown to grow with acetate (Campbell *et al.*, 2001; Miroshnichenko *et al.*, 2002; Pérez-Rodríguez *et al.*, 2010). Moreover, most *Nautiliales* are anaerobes or micro-aerophiles (Miroshnichenko *et al.*, 2002, 2004; Alain *et al.*, 2009; Pérez-Rodríguez *et al.*, 2010). The NautMG-group identified here is thus the first example of an aerobic, acetate-consuming member of the *Nautiliales*. Although we detected the NautMG-group as the only epsilonproteobacterial phylotype after the incubation, individual cells displayed remarkable differences in ^{13}C and ^{15}N uptake. The most parsimonious explanation is that during the multiple division cycles the cellular ^{13}C and ^{15}N content accumulated from generation to generation resulting in incrementally higher labeling of the daughter cells. However, quantitative data on cellular SI uptake after a FISH-SIMS protocol have to be cautiously interpreted as formaldehyde fixation and CARD-FISH can lead to an underestimation of SI uptake (Musat *et al.*, 2014).

Significance of acetate-consuming bacteria in diffuse fluids

Given the facts that acetate was not or not unambiguously measurable and that the enriched candidate heterotrophs were relatively rare in the source diffuse fluids, acetate-dependent heterotrophy likely played a minor role *in situ*. Accordingly, the pyrotag datasets indicated a prevalence of lithotrophic sulfur-oxidizers and thus a largely autotrophy-based microbial community. However, evidence is accumulating that geochemical properties, temperature and the microbial community composition of diffuse fluids at hydrothermal systems are highly dynamic in time and space (Perner *et al.*, 2013). The limited availability of organic carbon and the rapid dilution of venting fluids with seawater provide only a very narrow window, where conditions like temperature and substrate concentrations are favorable for heterotrophic growth. Consequently, microorganisms experience rapid changes in their immediate vicinity and require strategies to survive and to efficiently exploit temporarily available resources. We therefore propose that the observed quick cell growth upon acetate addition reflects an opportunistic, copiotrophic lifestyle of the NautMG-group and *Gammaproteobacteria* such as *Marinobacter* sp. as adaptation to the fluctuating conditions at hydrothermal vents. Here, the seawater bodies surrounding hydrothermal vents may serve as a reservoir for different heterotrophic microorganisms.

Outlook

While the detected acetate-assimilating populations were rare in the source diffuse fluids, these organisms might be more abundant in other compartments at hydrothermal vent systems. They could thrive at venting crack rims or in mussel beds, where conditions are less dynamic and concentrations of organic compounds may be higher. This would be in line with previous hypotheses that meso- and thermophiles in diffuse fluids are actually sessile organisms detached and flushed out from the subsurface by fluid venting (Summit & Baross, 2001; Huber *et al.*, 2003; Takai *et al.*, 2004). Further studies in other hydrothermal compartments are desirable to quantify the general importance of organic carbon turnover at hydrothermal vent sites. Future SI-labeling experiments should test a wider range of temperatures, oxygen concentrations, and other organic carbon sources such as formate, which is the major abiotically formed organic acid in hydrothermal fluids (McCollom & Seewald, 2001; Lang *et al.*, 2010). Additionally, SI-labeling experiments could be combined with transcriptomic and proteomic analyses to identify the involved metabolic pathways.

Acknowledgements

We thank the crew of the R/V *Meteor* and R/V *Sonne* and the ROV team of the MARUM Quest 4000 m. We greatly acknowledge the scientific parties, in particular the chief scientists Nicole Dubilier (cruise M83 leg 2) and Wolfgang Bach (cruise SO216) for their wonderful support. The cruises M82 with R/V *Meteor* and SO216 with R/V *Sonne* were integral parts of the Cluster of Excellence of the MARUM 'The Ocean in the Earth System, Research Area GB: Geosphere-Biosphere Interactions' funded by the German Research Foundation (DFG). We thank Marcus Petzold, Nicole Rödiger, Jörg Wulf, Lisa Drews, and Lisa Kieweg for excellent assistance in the Molecular Ecology department, Gabriele Klockgether for help with ISMS measurements, Marvin Dörries and Kathleen Trautwein for help with 2D-HPIC acetate measurements, and Andreas Krupke for support in the nanoSIMS analysis. The cruise SO216 was funded by a grant (03G0216) from the Bundesministerium für Bildung und Forschung (BMBF) awarded to Wolfgang Bach and co-PIs. This work was supported by the Max Planck Society.

Authors' contribution

M.W. and P.P. contributed equally to this study.

References

Alain K, Callac N, Guégan M, Lesongeur F, Crassous P, Cambon-Bonavita M-A, Querellou J & Prieur D (2009) *Nautilia abyssi* sp. nov., a thermophilic, chemolithoautotrophic, sulfur-reducing bacterium isolated from an East Pacific Rise hydrothermal vent. *Int J Syst Evol Microbiol* **59**: 1310–1315.

Albert DB, Taylor C & Martens CS (1995) Sulfate reduction rates and low molecular weight fatty acid concentrations in the water column and surficial sediments of the Black Sea. *Deep Sea Res A* **42**: 1239–1260.

Amend JP, Amend AC & Valenza M (1998) Determination of volatile fatty acids in the hot springs of Vulcano, Aeolian Islands, Italy. *Org Geochem* **28**: 699–705.

Bach W & Cruise Participants (2011) Report and preliminary results of RV SONNE Cruise SO-216, Townsville (Australia)-Makassar (Indonesia), June 14-July 23, 2011. BAMBUS, Back-Arc Manus Basin Underwater Solfataras. Reports, Faculty of Geosciences, University of Bremen: 280, 87 pp.

Bazylinski DA, Wirsen CO & Jannasch HW (1989) Microbial utilization of naturally occurring hydrocarbons at the Guaymas Basin hydrothermal vent site. *Appl Environ Microbiol* **55**: 2832–2836.

Berg C, Beckmann S, Jost G, Labrenz M & Jürgens K (2013) Acetate-utilizing bacteria at an oxic–anoxic interface in the Baltic Sea. *FEMS Microbiol Ecol* **85**: 251–261.

Boschker HTS, Nold SC, Wellsbury P, Bos D, de Graaf W, Pel R, Parkes RJ & Cappenberg TE (1998) Direct linking of microbial populations to specific biogeochemical processes by ^{13}C-labelling of biomarkers. *Nature* **392**: 801–805.

Bower CE & Holm-Hansen T (1980) A salicylate–hypochlorite method for determining ammonia in seawater. *Can J Fish Aquat Sci* **37**: 794–798.

Braman RS & Hendrix SA (1989) Nanogram nitrite and nitrate determination in environmental and biological materials by vanadium (III) reduction with chemiluminescence detection. *Anal Chem* **61**: 2715–2718.

Campbell BJ, Jeanthon C, Kostka JE, Luther GW & Cary SC (2001) Growth and phylogenetic properties of novel bacteria belonging to the epsilon subdivision of the *Proteobacteria* enriched from *Alvinella pompejana* and deep-sea hydrothermal vents. *Appl Environ Microbiol* **67**: 4566–4572.

Campbell BJ, Engel AS, Porter ML & Takai K (2006) The versatile ε-proteobacteria: key players in sulphidic habitats. *Nat Rev Microbiol* **4**: 458–468.

Charlou JL, Donval JP, Douville E, Jean-Baptiste P, Radford-Knoery J, Fouquet Y, Dapoigny A & Stievenard M (2000) Compared geochemical signatures and the evolution of Menez Gwen (37°50′N) and Lucky Strike (37°17′N) hydrothermal fluids, south of the Azores Triple Junction on the Mid-Atlantic Ridge. *Chem Geol* **171**: 49–75.

Charlou JL, Donval JP, Konn C, OndréAs H, Fouquet Y, Jean-Baptiste P & Fourré E (2010) High production and fluxes of H_2 and CH_4 and evidence of abiotic hydrocarbon synthesis by serpentinization in ultramafic-hosted hydrothermal systems on the Mid-Atlantic Ridge. *Diversity of Hydrothermal Systems on Slow Spreading Ocean Ridges*

(Rona PA, Devey CW, Dyment J. & Murton BJ, eds), pp. 265–296. American Geophysical Union, Washington, DC.

Cline JD (1969) Spectrophotometric determination of hydrogen sulfide in natural waters. *Limnol Oceanogr* **14**: 454–458.

Drake HL, Gößner AS & Daniel SL (2008) Old acetogens, new light. *Ann NY Acad Sci* **1125**: 100–128.

Grote J, Schott T, Bruckner CG, Glöckner FO, Jost G, Teeling H, Labrenz M & Jürgens K (2012) Genome and physiology of a model *Epsilonproteobacterium* responsible for sulfide detoxification in marine oxygen depletion zones. *P Natl Acad Sci USA* **109**: 506–510.

Handley KM, Héry M & Lloyd JR (2009) *Marinobacter santoriniensis* sp. nov., an arsenate-respiring and arsenite-oxidizing bacterium isolated from hydrothermal sediment. *Int J Syst Evol Microbiol* **59**: 886–892.

Ho T-Y, Scranton MI, Taylor GT, Varela R, Thunell RC & Muller-Karger F (2002) Acetate cycling in the water column of the Cariaco Basin: seasonal and vertical variability and implication for carbon cycling. *Limnol Oceanogr* **47**: 1119–1128.

Holm NG & Charlou JL (2001) Initial indications of abiotic formation of hydrocarbons in the Rainbow ultramafic hydrothermal system, Mid-Atlantic Ridge. *Earth Planet Sci Lett* **191**: 1–8.

Hoppe H-G (1978) Relations between active bacteria and heterotrophic potential in the sea. *Neth J Sea Res* **12**: 78–IN4.

Huber R, Stohr J, Hohenhaus S, Reinhard R, Burggraf S, Jannasch HW & Stetter KO (1995) *Thermococcus chitonophagus* sp. nov., a novel, chitin-degrading, hyperthermophilic archaeum from a deep-sea hydrothermal vent environment. *Arch Microbiol* **164**: 255–264.

Huber JA, Butterfield DA & Baross JA (2003) Bacterial diversity in a subseafloor habitat following a deep-sea volcanic eruption. *FEMS Microbiol Ecol* **43**: 393–409.

Huber JA, Mark Welch DB, Morrison HG, Huse SM, Neal PR, Butterfield DA & Sogin ML (2007) Microbial population structures in the deep marine biosphere. *Science* **318**: 97–100.

Ishii K, Mußmann M, MacGregor BJ & Amann R (2004) An improved fluorescence *in situ* hybridization protocol for the identification of bacteria and archaea in marine sediments. *FEMS Microbiol Ecol* **50**: 203–213.

Jeanthon C & Prieur D (1990) Susceptibility to heavy metals and characterization of heterotrophic bacteria isolated from two hydrothermal vent polychaete annelids, *Alvinella pompejana* and *Alvinella caudata*. *Appl Environ Microbiol* **56**: 3308–3314.

Karl DM, Taylor GT, Novitsky JA, Jannasch HW, Wirsen CO, Pace NR, Lane DJ, Olsen GJ & Giovannoni SJ (1988) A microbiological study of Guaymas Basin high temperature hydrothermal vents. *Deep Sea Res A* **35**: 777–791.

Karl DM, Brittain AM & Tilbrook BD (1989) Hydrothermal and microbial processes at Loihi Seamount, a mid-plate hot-spot volcano. *Deep Sea Res A* **36**: 1655–1673.

Kaye JZ & Baross JA (2000) High incidence of halotolerant bacteria in Pacific hydrothermal-vent and pelagic environments. *FEMS Microbiol Ecol* **32**: 249–260.

Kaye JZ, Sylvan JB, Edwards KJ & Baross JA (2011) *Halomonas* and *Marinobacter* ecotypes from hydrothermal vent, subseafloor and deep-sea environments. *FEMS Microbiol Ecol* **75**: 123–133.

Kirchman DL, Yu L, Fuchs BM & Amann R (2001) Structure of bacterial communities in aquatic systems as revealed by filter PCR. *Aquat Microb Ecol* **26**: 13–22.

Klindworth A, Pruesse E, Schweer T, Peplies J, Quast C, Horn M & Glöckner FO (2013) Evaluation of general 16S ribosomal RNA gene PCR primers for classical and next-generation sequencing-based diversity studies. *Nucleic Acids Res* **41**: e1.

Konn C, Charlou JL, Donval JP, Holm NG, Dehairs F & Bouillon S (2009) Hydrocarbons and oxidized organic compounds in hydrothermal fluids from Rainbow and Lost City ultramafic-hosted vents. *Chem Geol* **258**: 299–314.

La Duc MT, Benardini JN, Kempf MJ, Newcombe DA, Lubarsky M & Venkateswaran K (2007) Microbial diversity of Indian Ocean hydrothermal vent plumes: microbes tolerant of desiccation, peroxide exposure, and ultraviolet and γ -irradiation. *Astrobiology* **7**: 416–431.

Lanave C, Preparata G, Saccone C & Serio G (1984) A new method for calculating evolutionary substitution rates. *J Mol Evol* **20**: 86–93.

Lang SQ, Butterfield DA, Schulte M, Kelley DS & Lilley MD (2010) Elevated concentrations of formate, acetate and dissolved organic carbon found at the Lost City hydrothermal field. *Geochim Cosmochim Acta* **74**: 941–952.

Lee S & Fuhrman JA (1987) Relationships between biovolume and biomass of naturally derived marine bacterioplankton. *Appl Environ Microbiol* **53**: 1298–1303.

Lever M, Heuer V, Morono Y, Masui N, Schmidt F, Alperin M, Inagaki F, Hinrichs K-U & Teske A (2010) Acetogenesis in deep subseafloor sediments of the Juan de Fuca ridge flank: a synthesis of geochemical, thermodynamic, and gene-based evidence. *Geomicrobiol J* **27**: 183–211.

Ludwig W, Strunk O, Westram R *et al.* (2004) ARB: a software environment for sequence data. *Nucleic Acids Res* **32**: 1363–1371.

Marcon Y, Sahling H, Borowski C, dos Santos Ferreira C, Thal J & Bohrmann G (2013) Megafaunal distribution and assessment of total methane and sulfide consumption by mussel beds at Menez Gwen hydrothermal vent, based on geo-referenced photomosaics. *Deep Sea Res A* **75**: 93–109.

Marteinsson V, Birrien J-L, Kristjánsson JK & Prieur D (1995) First isolation of thermophilic aerobic non-sporulating heterotrophic bacteria from deep-sea hydrothermal vents. *FEMS Microbiol Ecol* **18**: 163–174.

McCollom TM & Seewald JS (2001) A reassessment of the potential for reduction of dissolved CO_2 to hydrocarbons during serpentinization of olivine. *Geochim Cosmochim Acta* **65**: 3769–3778.

McCollom TM & Seewald JS (2007) Abiotic synthesis of organic compounds in deep-sea hydrothermal environments. *Chem Rev* **107**: 382–401.

Miroshnichenko ML, Kostrikina NA, L'Haridon S, Jeanthon C, Hippe H, Stackebrandt E & Bonch-Osmolovskaya EA (2002) *Nautilia lithotrophica* gen. nov., sp. nov., a thermophilic sulfur-reducing epsilon-proteobacterium isolated from a deep-sea hydrothermal vent. *Int J Syst Evol Microbiol* **52**: 1299–1304.

Miroshnichenko ML, L'Haridon S, Schumann P, Spring S, Bonch-Osmolovskaya EA, Jeanthon C & Stackebrandt E (2004) *Caminibacter profundus* sp. nov., a novel thermophile of *Nautiliales* ord. nov. within the class "*Epsilonproteobacteria*", isolated from a deep-sea hydrothermal vent. *Int J Syst Evol Microbiol* **54**: 41–45.

Miyatake T, MacGregor BJ & Boschker HTS (2013) Depth-related differences in organic substrate utilization by major microbial groups in intertidal marine sediment. *Appl Environ Microbiol* **79**: 389–392.

Musat N, Halm H, Winterholler B, Hoppe P, Peduzzi S, Hillion F, Horreard F, Amann R, Jørgensen BB & Kuypers MMM (2008) A single-cell view on the ecophysiology of anoxic phototrophic bacteria. *P Natl Acad Sci USA* **105**: 17861–17866.

Musat N, Stryhanyuk H, Bombach P, Adrian L, Audinot JN & Richnow HH (2014) The effect of FISH and CARD-FISH on the isotopic composition of ^{13}C- and ^{15}N-labeled *Pseudomonas putida* cells measured by nanoSIMS. *Syst Appl Microbiol* **37**: 267–276.

Muyzer G, Teske A, Wirsen C & Jannasch HW (1995) Phylogenetic relationships of *Thiomicrospira* species and their identification in deep-sea hydrothermal vent samples by denaturing gradient gel electrophoresis of 16S rDNA fragments. *Arch Microbiol* **164**: 165–172.

Muyzer G, Brinkhoff T, Nübel U, Santegoeds C, Schäfer H & Wawer C (1998) Denaturing gradient gel electrophoresis (DGGE) in microbial ecology. *Molecular Microbial Ecology Manual*, pp. 3.4.4/1–3.4.4/27. Kluwer Academic Publishers, Dordrecht, the Netherlands.

Nakagawa S & Takai K (2008) Deep-sea vent chemoautotrophs: diversity, biochemistry and ecological significance. *FEMS Microbiol Ecol* **65**: 1–14.

Pérez-Rodríguez I, Ricci J, Voordeckers JW, Starovoytov V & Vetriani C (2010) *Nautilia nitratireducens* sp. nov., a thermophilic, anoxic, chemosynthetic, nitrate-ammonifying bacterium isolated from a deep-sea hydrothermal vent. *Int J Syst Evol Microbiol* **60**: 1182–1186.

Perner M, Gonnella G, Hourdez S, Böhnke S, Kurtz S & Girguis P (2013) *In situ* chemistry and microbial community compositions in five deep-sea hydrothermal fluid samples from Irina II in the Logatchev field. *Environ Microbiol* **15**: 1551–1560.

Pernthaler A, Pernthaler J & Amann R (2004) Sensitive multi-color fluorescence *in situ* hybridization for indentification of environmental microorganisms. *Molecular Microbial Ecology Manual* (Kowalchuk GA, de Bruijn FJ, Head IM, Van der Zijpp AJ & van Elsas JD, eds), pp. 711–726. Kluwer Academic Publishers, Dodrecht.

Pester M, Bittner N, Deevong P, Wagner M & Loy A (2010) A "rare biosphere" microorganism contributes to sulfate reduction in a peatland. *ISME J* **4**: 1591–1602.

Pimenov NV, Kaliuzhnaia MG, Khmelenina VN, Mitiushina LL & Trotsenko IA (2002) Utilization of methane and carbon dioxide by symbiotrophic bacteria in gills of *Mytilidae* (*Bathymodiolus*) from the Rainbow and Logachev hydrothermal fields on the Mid-Atlantic Ridge. *Mikrobiologiia* **71**: 681–689.

Pley U (1991) *Pyrodictium abyssi* sp. nov. represents a novel heterotrophic marine archaeal hyperthermophile growing at 110 °C. *Syst Appl Microbiol* **14**: 245–253.

Polerecky L, Adam B, Milucka J, Musat N, Vagner T & Kuypers MMM (2012) LOOK@NANOSIMS – a tool for the analysis of nanoSIMS data in environmental microbiology. *Environ Microbiol* **14**: 1009–1023.

Pruesse E, Peplies J & Glöckner FO (2012) SINA: accurate high-throughput multiple sequence alignment of ribosomal RNA genes. *Bioinformatics* **28**: 1823–1829.

Quast C, Pruesse E, Yilmaz P, Gerken J, Schweer T, Yarza P, Peplies J & Glöckner FO (2013) The SILVA ribosomal RNA gene database project: improved data processing and web-based tools. *Nucleic Acids Res* **41**: D590–D596.

Raguénès G, Pignet P, Gauthier G, Peres A, Christen R, Rougeaux H, Barbier G & Guezennec J (1996) Description of a new polymer-secreting bacterium from a deep-sea hydrothermal vent, *Alteromonas macleodii* subsp. *fijiensis*, and preliminary characterization of the polymer. *Appl Environ Microbiol* **62**: 67–73.

Reeves EP, Prieto X, Hentscher M, Rosner M, Seewald J, Hinrichs KU & Bach W (2011) Phase separation, degassing and anomalous methane at the Menez Gwen hydrothermal field. Mineralogical Magazine, 75, p1702 (abstract). 21st Annual V.M. Goldschmidt Conference, Prague.

Reeves EP, McDermott JM & Seewald JS (2014) The origin of methanethiol in midocean ridge hydrothermal fluids. *P Natl Acad Sci USA* **111**: 5474–5479.

Rogers KL & Amend JP (2006) Energetics of potential heterotrophic metabolisms in the marine hydrothermal system of Vulcano Island, Italy. *Geochim Cosmochim Acta* **70**: 6180–6200.

Rogers DR, Santelli CM & Edwards KJ (2003) Geomicrobiology of deep-sea deposits: estimating community diversity from low-temperature seafloor rocks and minerals. *Geobiology* **1**: 109–117.

Santelli CM, Orcutt BN, Banning E, Bach W, Moyer CL, Sogin ML, Staudigel H & Edwards KJ (2008) Abundance and diversity of microbial life in ocean crust. *Nature* **453**: 653–656.

Schmidt K, Koschinsky A, Garbe-Schönberg D, de Carvalho LM & Seifert R (2007) Geochemistry of hydrothermal fluids from the ultramafic-hosted Logatchev hydrothermal field, 15°N on the Mid-Atlantic Ridge: temporal and spatial investigation. *Chem Geol* **242**: 1–21.

Shively JM, van Keulen G & Meijer WG (1998) Something from almost nothing: carbon dioxide fixation in chemoautotrophs. *Annu Rev Microbiol* **52**: 191–230.

Shock EL & Schulte MD (1998) Organic synthesis during fluid mixing in hydrothermal systems. *J Geophys Res Planets* **103**: 28513–28527.

Sievert SM, Wieringa EBA, Wirsen CO & Taylor CD (2007) Growth and mechanism of filamentous-sulfur formation by *Candidatus* Arcobacter sulfidicus in opposing oxygen-sulfide gradients. *Environ Microbiol* **9**: 271–276.

Sievert SM, Hügler M, Taylor CD & Wirsen CO (2008) Sulfur oxidation at deep-sea hydrothermal vents. *Microbial Sulfur Metabolism* (Dahl DC & Friedrich DCG, eds), pp. 238–258. Springer, Berlin, Heidelberg.

Stamatakis A, Ludwig T & Meier H (2005) RAXML-III: a fast program for maximum likelihood-based inference of large phylogenetic trees. *Bioinformatics* **21**: 456–463.

Summit M & Baross JA (2001) A novel microbial habitat in the mid-ocean ridge subseafloor. *P Natl Acad Sci USA* **98**: 2158–2163.

Takai K, Gamo T, Tsunogai U, Nakayama N, Hirayama H, Nealson KH & Horikoshi K (2004) Geochemical and microbiological evidence for a hydrogen-based, hyperthermophilic subsurface lithoautotrophic microbial ecosystem (HyperSLiME) beneath an active deep-sea hydrothermal field. *Extremophiles* **8**: 269–282.

Teira E, Reinthaler T, Pernthaler A, Pernthaler J & Herndl GJ (2004) Combining catalyzed reporter deposition-fluorescence *in situ* hybridization and microautoradiography to detect substrate utilization by bacteria and archaea in the deep ocean. *Appl Environ Microbiol* **70**: 4411–4414.

Tuttle AJ (1985) The role of sulfur-oxidizing bacteria at deep-sea hydrothermal vents. *Bull Biol Soc Wash* **6**: 335–343.

Tuttle JH, Wirsen CO & Jannasch HW (1983) Microbial activities in the emitted hydrothermal waters of the Galápagos rift vents. *Mar Biol* **73**: 293–299.

Vandieken V, Pester M, Finke N, Hyun J-H, Friedrich MW, Loy A & Thamdrup B (2012) Three manganese oxide-rich marine sediments harbor similar communities of acetate-oxidizing manganese-reducing bacteria. *ISME J* **6**: 2078–2090.

Wang Y, Yang J, Lee OO, Dash S, Lau SCK, Al-Suwailem A, Wong TYH, Danchin A & Qian P-Y (2011) Hydrothermally generated aromatic compounds are consumed by bacteria colonizing in Atlantis II Deep of the Red Sea. *ISME J* **5**: 1652–1659.

Wankel SD, Germanovich LN, Lilley MD, Genc G, DiPerna CJ, Bradley AS, Olsen EJ & Girguis PR (2011) Influence of subsurface biosphere on geochemical fluxes from diffuse hydrothermal fluids. *Nat Geosci* **4**: 461–468.

Wood AP, Aurikko JP & Kelly DP (2004) A challenge for 21st century molecular biology and biochemistry: what are the causes of obligate autotrophy and methanotrophy? *FEMS Microbiol Rev* **28**: 335–352.

Wright RR & Hobbie JE (1966) Use of glucose and acetate by bacteria and algae in aquatic ecosystems. *Ecology* **47**: 447–464.

Yamamoto M & Takai K (2011) Sulfur metabolisms in epsilon- and gamma-*Proteobacteria* in deep-sea hydrothermal fields. *Front Microbiol* **2**: 192.

Supporting Information

Additional Supporting Information may be found in the online version of this article:

Table S1. Descriptive statistics of bacterial 16S rRNA gene 454-pyrosequences.

Table S2. Oligonucleotide probes applied in this study.

Table S3. TCC and CARD-FISH results in diffuse fluids and in incubation experiments.

Table S4. Bulk ^{13}C- and ^{15}N-content determined by IRMS in oxic and anoxic incubations and acetate-free control incubations given as mean AT% (AT% $^{13}C = (^{13}C/(^{13}C + ^{12}C)) \times 100$ and as mean AT% $^{15}N = (^{15}N/(^{15}N + ^{14}N)) \times 100$).

Fig. S1. Upper panel: sampling sites of this study (red dots). Lower left panel: Woody Crack (WC) with associated fauna (*Bathymodiolus* mussels, crabs). Middle panel: North Su (NS) with ROV-arm holding KIPS system and a coupled temperature sensor. Right panel: tube worms at Fenway (FW).

Fig. S2. Bulk ^{13}C- and ^{15}N-content of oxic acetate incubations and dead controls given in AT% (AT% $^{13}C = (^{13}C/(^{13}C + ^{12}C)) \times 100$; and AT% $^{15}N = (^{15}N/(^{15}N + ^{14}N)) \times 100$).

Fig. S3. NanoSIMS analysis of ^{13}C-acetate and ^{15}N-ammonium uptake by single cells in incubation experiments with North Su-IIa fluids (NS-IIa, 72 °C) from Manus Basin.

Fig. S4. Comparison of labeling of individual cells in ^{13}C-acetate (AT% $^{13}C = (^{13}C/(^{13}C + ^{12}C)) \times 100$) vs. ^{15}N-ammonium (AT% $^{15}N = (^{15}N/(^{15}N + ^{14}N)) \times 100$) from incubation experiments analyzed by nanoSIMS.

Methods S1. 16S rRNA gene libraries, 454-pyrotag sequencing and probe design.